BIOCHEMISTRY

 Volume 44, Number 46 November 22, 2005

Articles

Site-Directed Fluorescence Labeling Reveals Differences on the R-Conformer of Glucosamine 6-Phosphate Deaminase of *Escherichia coli* Induced by Active or Allosteric Site Ligands at Steady State†

Alejandro Sosa-Peinado* and Martín González-Andrade

Departamento de Bioquímica, Facultad de Medicina, Universidad Nacional Autónoma de México, P.O. Box 70-159, México, D.F. 04510, México

Received February 18, 2005; Revised Manuscript Received September 8, 2005

ABSTRACT: Engineered glucosamine 6-phosphate deaminase of *Escherichia coli* with unique reactive cysteines at positions 164 or 206 was created by site-directed mutagenesis to monitor the allosteric transition in solution by the fluorescence emission of the bimane or dansyl-amidoethyl groups attached to the indicated residues. The selection of both positions was due to the differential interaction of these residues between T- and R-conformers at the interface of two trimers that form the hexameric structure; in the T-conformer, residue 164 or 206 presents only intrasubunit contacts, but in the R-conformer, new intersubunit contacts are established. As in the wild-type enzyme, fluorescent-labeled mutants show no modification on the allosteric activation of the *K*-system, only the k_{cat} was reduced to a value of 72 s^{-1} (~50% of wild-type). With these preparations, conformational changes were detected by the fluorescence emission spectra at steady state when the active site or the allosteric site ligands were titrated. Despite the similar changes in the fluorescence spectra that were correlated with the induction of the R-state, differences were observed at the maximal change in the fluorescence spectra and in the relative solvent polarities at the positions labeled. These data suggested structural differences in the conformation of the R-state when it is induced from the active site or from the allosteric site, which is not consistent with the two-state structural model proposed by previous crystallographic studies of this enzyme.

Conformational flexibility in allosteric proteins plays a fundamental role for understanding the changes in the affinity of ligands during the propagation of multiple conformational changes throughout the molecule (*1*). Evidences mainly from thermodynamics (*2*), nuclear magnetic resonance (NMR, *3*), and spectroscopical studies (*4*) proposed that several allosteric transitions could be described as a dynamic equilibrium between conformers, in which the conformational change may be driven by conformer stabilization from preexisting equilibrium after ligand binding. NMR techniques have revealed motions accounted by proteins during ligand binding or catalysis (*5*). However, oligomeric enzymes are usually not amenable to these studies; therefore, it is fundamental to develop systems to study the dynamics of oligomeric enzymes in solution.

Site-directed labeling (SDL)[1] methods by fluorescent or spin labels have emerged as a powerful technique to obtain

† This work was partially supported by Grant IN5582E from DGAPA of National Autonomous University of México (UNAM) and Grants IN213301 and 41328 from the National Council of Science and Technology (CONACyT, México). M.G.-A. is a recipient of the fellowship for Ph.D. studies from CONACyT, México and DGAPA-UNAM.

* To whom correspondence should be addressed. Phone, (525) 623-2275; fax, (525) 623-2419; e-mail, asosa@bq.unam.mx.

10.1021/bi050306o CCC: $30.25
Published on Web 10/28/2005

structural information of proteins in solution (*6*−*9*). These methods are based on the correlation of physicochemical parameters of the labels introduced at specific sites of a protein with solvent accessibility, solvent polarity, or mobility. These techniques (SDL) have allowed the detection of secondary structure motifs of a protein, movements among different regions, and the generation of a three-dimensional structural model of a membrane-bound protein (*9*). In particular, chemical modification of T4 lysozyme (*6*, *7*) with monobromobimane (mBBr, about the size of trypthophan after incorporation to the protein) has several advantages: it does not perturb protein stability of exposed sites to the solvent; energy destabilization ($\Delta\Delta G$) $\leq$ 1.5 kcal is obtained when residues are exposed to the solvent $\geq$40 Å^2 (*6*); and solvent accessibility is correlated with λ_{max} of fluorescence emission and steady-state anisotropy values (*6*, *7*). In addition, trypthophan is able to quench the fluorescence of bimane when the distance between them is $\leq$6 Å (*7*).

Here, we used as a model the allosteric transition carried out by glucosamine 6-P deaminase of *Escherichia coli* (EC 3.5.99.6). This enzyme catalyzes the reversible conversion of D-glucosamine 6-phosphate (GlcN6P) into D-fructose-phosphate and ammonia, and it is allosterically activated by *N*-acetylglucosamine 6-phosphate (GlcNac6P), the allosteric site ligand (*10*−*12*). The three-dimensional structures of the enzyme in the R-conformer and in the T-conformer have been obtained at resolutions between 1.9 and 2.2 Å (*13*, *14*). The enzyme is a homo-hexamer arranged as a dimer of trimers with a 32 internal symmetry. Active sites are located at the crevice in each identical subunit, and the allosteric sites are located in the clefts adjacent to each subunit around the three-fold axes of the molecule (*13*, *14*). The crystallographic structure of the R-conformer is invariant in the presence of the active site ligand (in the presence of inorganic phosphate, *13*) or in the presence of the allosteric ligand; the crystallization of the enzyme only in the presence of the active site ligand is never achieved (*13*, *14*). Since phosphate binds to the allosteric site, it may obscure the effect of the active site ligand in the formation of the R-state. Furthermore, Arg158 and Lys160 of one monomer, together with the N-terminal of the neighboring subunit, bind to the phosphate moiety of the allosteric activator in the R-conformer. Hence, site-directed labeling (SDL) was used to test if the R′-conformer induced from the active site is able to generate a similar conformer to the one induced from the allosteric site without stabilization of the adjacent positive charges present at the allosteric site (*13*, *14*). The idea of two structural different R-conformers, one induced by the active site ligand (R′) and other (R) generated from allosteric site ligand, is schematized in Figure 1. Despite the kinetic constants for GlcN6P deaminase of *E. coli* being satisfactorily described by the symmetry model of Monod−Wayman−Changuex, this does not exclude the presence of more than two-state structural conformers, as indicated by a new paradigm for the study of the regulation of allosteric enzymes (*15*, *16*).

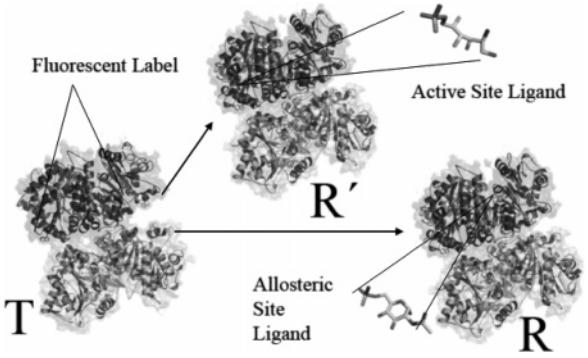

FIGURE 1: Schematic representation of the differences on the R-conformer induced from the allosteric site and the R′-conformer induced from the active site for the GlcN6P deaminase of *E. coli*. The structure of the enzyme is represented in a surface model in combination of the three-dimensional structure. The models were created with protein data bank files 1fs6 (T-conformer) and 1frz (R-conformer) with the PyMOL program (*23*).

Labeled mutants of GlcN6P deaminase of *E. coli* with mBBr or dansyl-amidoethyl-MTS at position 164 or 206 showed an allosteric activation *K*-type pattern as in the wild-type enzyme (*11*). Fluorescence changes at the interface of two trimers upon addition of the active or the allosteric ligands correlated with enzyme kinetics. Also, changes in the fluorescence spectra and solvent polarity were analyzed in terms of the different microenvironment interaction of residue 164 or 206 observed at the crystallographic structures. The changes on the fluorescence spectra at steady state were taken as an evidence of the differences in the quaternary changes associated to the formation of the R-state from the active or from the allosteric site. The work presented here illustrates the advantage of using site-directed fluorescence labeling for probing the conformational dynamics of a relatively large allosteric enzyme like GlcN6P deaminase in solution.

MATERIALS AND METHODS

Chemicals. Most chemical and biochemical reagents were from Sigma Aldrich S.A. de C.V., Mexico. Fluorescent labels bromobimane (mBBr) and dansyl-amidoethyl methanethiosulfonate (dansyl-amidoethyl-MTS) were purchased from Toronto Chemical Research (Toronto, Canada). The affinity gel used for GlcN6P deaminase purification (*N*-aminohexanoyl-glucosamine-6-P agarose) was prepared as described (*10*) except that ECH-Sepharose (Pharmacia) was used. The allosteric activator GlcNAc6P was prepared as described (*11*). Preparation of the competitive inhibitor GlcN-ol-6P was synthesized as described (*11*) by reduction of GlcN6P with $NaBH_4$.

Strains and Plasmid. Wild-type and mutants of GlcN6-P deaminase were prepared from a strain of *E. coli* carrying a

[1] Abbreviations: 164C-GlcN6P deaminase, mutant C118S/C228S/C239S/S164C of glucosamine 6-P deaminase; 206C-GlcN6P deaminase, mutant C118S/C228S/C239S/S206C of glucosamine 6-P deaminase; bimane-164C-GlcN6P deaminase, mutant C118S/C228S/C239S/S164C of glucosamine 6-P deaminase labeled with monobromobimane; dansyl-amidoethyl-164C-GlcN6P deaminase, mutant C118S/C228S/C239S/S164C of glucosamine 6-P deaminase chemically modified with dansyl-amidoethyl-MTS; bimane-206C-GlcN6P deaminase, mutant C118S/C228S/C239S/S206C of glucosamine 6-P deaminase chemically modified with monobromobimane; dansyl-amidoethyl-206C-GlcN6P deaminase, mutant C118S/C228S/C239S/S206C of glucosamine 6-P deaminase chemically modified with dansyl-amidoethyl-MTS; dansyl-amidoethyl-MTS (dansyl-amidoethyl methanethiosulfonate), 2-5-dimethylaminonaphthyl-1-sulfonamido ethyl methanethiosulfonate; DTNB, 5,5′-dithiobis(2-nitrobenzoic acid); GlcN-ol-6P, 2-deoxy-2-aminoglucitol 6-phosphate; GlcN6P, glucosamine 6-phosphate; GlcNAc6P, *N*-acetyl-glucosamine-6-phosphate; GlcN6P deaminase, glucosamine 6-phosphate deaminase; λ_{max}, fluorescence emission maxima; mBBr, monobromobimane; SDL, site-directed labeling.

plasmid (pTZ18R), which contains the deaminase gene of *E. coli* (nagB) for expression of the protein from the *lac* promoter as described (*11*, *17*). Similar plasmids expressing mutated sequences were constructed on the same vector. The host strain for protein expression was *E. coli* IBPC590, where expression of the chromosomal copy of the nagB gene was eliminated by insertion of a kanamycin-resistance cassette (*17*). IBPC590 is in addition Δ*lacI*; therefore, the expression of deaminase is constitutive.

Mutagenesis. Site-directed mutagenesis for the elimination of three cysteines (substituted by serines) was done by a successive single-directed mutagenesis from the wild-type plasmid in the following order: 118, 228, and 239. Creation of unique reactive cysteines was done from a plasmid encoding the triple mutant C118S/C228S/C239S. Site-directed mutagenesis was carried out with the Quick change kit (Stratagene, La Jolla, CA) following vendor specifications. The amount of plasmid (containing the gene encoding GlcN6P deaminase) pTZ18R*nagB* was 50 ng, and the amount of mutagenic oligonucleotides was 125 ng. PCR amplification included 25 cycles of denaturation at 95 °C for 1 min, annealing at 55 °C for 1 min, and polymerization at 68 °C for 10 min, followed by one final extension step at 68 °C for 10 min. Oligonucleotides used to create the single mutant C118S were 5′-GACGCCGAGAGCCGCCAGTAT-3′ and 5′-ATACTGGCGGCTCTCGGCGTC-3′; for the double mutant C118S/C228S, 5′-ACCATCAGCAGT CTGCAACTGC-3′ and 5′-GCAGTTGCAGGCTGATGGT-3′; and for the triple mutant C118S/C228S/C239S, 5′-ATCATGGTGAGC-GATGAACCTTC-3′ and 5′-GAAGGTTCATC GCTCAC-CATGAT-3′. For creation of the unique reactive cysteine at position 164 (C118S/C228S/C239S/H164C), oligonucleotides were 5'-TATCAAAACCCTGACTTGCGACACTC-3 and 5'-AGTGTCGCAAGTCAGGGTTTTGATAC-3, and for the creation of the unique reactive cysteine at position 206 (C118S/C228S/C239S/S206C), 5′-CGCTGGGTTGCCAGA-AAGCAC-3′ and 5′-GTGCTTTCTGGCAACCCAGC-3′. After the mutagenesis experiments, the products of PCR amplification were digested with DpnI enzyme and transformed in competent XL1-blue cells. The sequences of all constructs were corroborated with an ABI PRISM 310 Genetic Analyzer (Perkin-Elmer Applied Biosystems) at the sequencing facility of Instituto de Fisiologia Celular, UNAM, México.

Protein Expression and Purification of the Wild-type Enzyme and the Mutants. Protein expression in strain IBPC590 is constitutive; temperature for expression was selected at 30 °C. GlcN6P deaminase was purified as previously reported (*10*) using allosteric site-affinity chromatography. Mutants were purified following the same procedure. The purity of the preparations was verified by SDS−polyacrylamide gel electrophoresis (12%) with a yield higher than 98% as judged by densitometry analysis of the Coomassie blue-stained gel.

Protein Concentration. Concentrations of wild-type enzyme and mutant enzymes before labeling were calculated from their absorbance at 279 nm in 50 mM Tris-HCl (pH 7.5), using the known molar absorptivity of 20.02×10^4 M^{-1} cm^{-1} (*10*, *11*). Concentration data always refer to the hexameric protein. Protein concentrations of mutants chemically modified with mBBr and dansyl-amidoethyl-MTS were measured with the bicinchoninic method (*18*), using wild-type protein as standard. mBBr-labeled protein concentrations were estimated using the molar absorptivity at 380 nm of 5000 M^{-1} cm^{-1} (*19*).

Enzyme Assays. GlcN6P deaminase activity was assayed in the direction of fructose-6P formation by the colorimetric measurement of fructose at fixed times as previously reported (*10*). The progress of the reaction was always kept below 5% conversion of the initial substrate. Measurements were made in 50 mM Tris-HCl (pH 7.5), at 30 °C. Kinetic data were analyzed with the nonlinear regression subroutine of the program Origin 7 (MicroCal Software, Inc., Northampton, MA). The experimental data obtained were fitted to the MWC equation (*12*, *20*).

$$v_0 = \frac{k_{cat} n [E_t][Lc\alpha(1 + c\alpha)^{n-1} + \alpha(1 + \alpha)^{n-1}]}{L(1 + c\alpha)^n + (1 + c\alpha)^n} \quad (1)$$

Where α is normalized substrate concentration [GlcN6P/K_m^R], L is the ratio between the two conformers T/R, and c is the ratio of the dissociation constants for the R- and T-states (K_R/K_T); [E_t] is the concentration for the hexameric protein.

Chemical Modification of Unique Reactive Cysteines at Position 164 or 206 with mBBr and Dansyl-amidoethyl-MTS and Binding Efficiency. Labeling of purified mutants of GlcN6P deaminase at unique reactive cysteine positions 164 or 206 was carried out with a 10× molar excess of fluorophores dissolved in 20% DMSO (v/v), with a final concentration of the organic solvent not higher than 5% (v/v) to avoid protein denaturation. To carry out the complete chemical modification, the samples were incubated in 50 mM Tris-HCl (pH 7.5) at 4 °C for 12 h (overnight). Protein concentrations used during the chemical modification procedures varied between 5 and 10 mg/mL. Previous to labeling, protein samples were reduced with 1 mM DTT (in 50 mM Tris-HCl, pH 7.5, 1 h a 4 °C), followed by gel filtration in an HR-100 column (Pharmacia, Biotech) to eliminate the excess of DTT. After chemical modification, the excess of the label was removed by successive protein concentration and dilution with an Amicon Ultra-4 filter device (10 kDa of cutoff), for at least 10 000 times of dilution factor for complete removal of the excess of label. Labeling efficiency was tested by the reactivity of the protein to 5-5′-dithiobis (2-nitrobenzoic) acid (DTNB, *21*), by measuring the release of 2-nitrobenzoate (TNB). Incubation of the triple mutant C118S/C228S/C239S in its native state showed that the level of background labeling was less than 1%, as judged by the fluorescence of mBBr spuriously bound to the protein.

Fluorescence Determinations at Steady State. Fluorescence emission at steady state was carried out on an ISS PC1 spectrofluorometer (ISS Inc., Champine, IL); the temperature of the samples was equilibrated at 30 °C with a water bath, using 1 μM of final enzyme concentration in 50 mM Tris-HCl (pH7.5). Excitation wavelength for mBBr-labeled proteins was 381 nm and for dansyl-amidoethyl-MTS-labeled proteins was 341 nm. The band-passes for excitation and emission were 4 and 8 nm, respectively. The fluorescence emission spectra at saturation of ligands were measured from 400 to 600 nm, with an integration time of 1 s and a step size of 1 nm. Titrations of ligands measured by fluorescence emission spectra were collected for bimane- or dansyl-amidoethyl-labeled proteins from 450 to 500 nm or from

Table 1: Kinetic Parameters of Triple Mutant C118S/C228S/C239S of GlcN6P Deaminase and Wild-type Enzyme of *E. coli*

	k_{cat} (s^{-1})[a]	K_M (mM)[b]	$K_{0.5GlcN6P}$ (mM)[c]	k_{cat}/K_M	L ($\times 10^6$)[d]	c[d]	$K_{i\ GlcN-ol-6P}$ (μM)[e]
wild-type GlcN6P deaminase	153 ± 0.08	0.5 ± 0.04	5.2 ± 0.04	1.43×10^5	1.0 ± 0.04	0.02 ± 0.002	2.23 ± 0.4
C118S/C228S/C239S GlcN6P deaminase	96 ± 0.06	0.46 ± 0.07	5.1 ± 0.06	2.23×10^5	0.8 ± 0.05	0.022 ± 0.005	4.3 ± 0.2

[a] Data calculated from the fitted MWC model (*20*) by nonlinear regression. [b] Data calculated from the fitted Michaelis−Menten equation in saturating concentrations of the allosteric activator. [c] Data calculated from the fitted Hill equation in absence of the allosteric activator. [d] Data calculated from the fitted MWC equation in the absence of the allosteric activator. [e] Data calculated from the fitted linear competitive equation in the presence of 2 mM of the activator. All constants and deviations standards were calculated from al least three experiments.

450 to 550 respectively, with an integration time of 3 s and a step size of 0.5 nm. The λ_{max} of the emission spectra was calculated from the first derivate of the spectra. Protein modified with dansyl-amidoethyl-MTS required approximately 20 min to stabilize a drift in basal fluorescence emission before the addition of ligands.

Relative Solvent Polarity Determinations with Bimane−Cysteine and Dansyl-amidoethyl−Cysteine. Correlation curves for fluorophores attached to cysteine with solvent polarity was carried out by reacting mBBr (30 μM) or dansyl-amidoethyl-MTS (30 μM) with L-cysteine (150 μM), and then measuring the fluorescence emission spectra in dioxane/water mixtures that ranged from 0 to 100% (v/v) of dioxane at 30 °C. For fluorescence emission calibration, final concentration of fluorophores attached to cysteine was 1 μM, in 50 mM Tris-HCl (pH7.5).

Quantum Yield Measurements. The quantum yield of mBBr- or dansyl-amidoethyl-MTS-labeled proteins and the intrinsic fluorescence of the wild-type enzyme were measured as described (*22*), using quinine sulfate (quantum yield equal to 0.55 in 1 N H_2SO_4) as standard. Corrected emission spectra for the different fluorophores were collected at different intervals: for quinine sulfate was from 370 to 700 nm (360 nm of λ_{exc}), for wild-type protein was from 305 to 450 nm (295 nm of λ_{exc}), for dansyl-amidoethyl-labeled proteins were from 350 to 700 nm (341 nm of λ_{exc}), and for bimane-labeled proteins were from 391 to 700 nm (381 nm of λ_{exc}). Basal buffer fluorescence was subtracted from each sample before quantum yield.

Molecular Visualization and Analysis of Structural Differences between T- and R-Conformer. Molecular models and figures were created with PyMOL program (*23*). Introduction of trypthophan at position 164 or 206 (mutation in silico) was done by choosing a rotamer of trypthophan with lowest energy into the protein data bank (PDB) file of the hexameric T-conformer (1fs6) and R-conformer (1frz), from the PyMOL program rotamer library. After trypthophan replacement into the structure file of each conformer, the CHARMM energy function algorithm (*24*) was used to minimize the rotamer conformation of the introduced trypthophan. Minimizations were performed using the program CHARMM Beta Release Version 28b1 on a Linux-2.4.20-8 (i686) 1.5 GHz Athlon CPUs, by the adopted basic Newton−Raphson (ABNR) method, using 500 cycles of minimization. Calculation of the solvent accessible surface areas from the PDB files on the T- or R-conformer was done by the NACCESS program that use the algorithm of Richard (*25*), considering a radius of the probe of 1.4 Å.

RESULTS

Wild-type GlcN6P Deaminase and Triple Mutant C118S/C228S/C239S Behave as Allosteric System of K-type. From the four residues of cysteine per monomer in the wild-type enzyme (118, 228, 219, and 239), two react with thiol reagents in the T-conformation (positions 118 and 239), while the reactivity for thiols is completely protected in the R-conformation (*26*). However, these cysteines were not suitable for monitoring conformational changes by SDL, because of a notably reduction in the activity after chemical modification. Nevertheless, it has been reported that replacement of cysteine 118 and/or 239 by serine does not modify allosteric activation of *K*-type (*26*). Therefore, to eliminate the unwanted reactivity of thiol groups during fluorescent labeling, three of these cysteines were replaced by serine (C118S/C228S/C239S). The triple mutant was not reactive to DTNB in the native state, since the only residue of cysteine present (position 219) is at the center of the hexameric structure and is probably forming a disulfide bond, as evidenced by crystallographic studies (*13*). Table 1 shows the kinetic parameters of the wild-type and the triple mutant C118S/C228S/C239S of the enzyme. The triple mutant was active and exhibited a positive homotropic and positive heterotropic activation of *K*-type for the deaminase reaction: the $K_{0.5}$ for substrate decreased at higher concentrations of the allosteric ligand (in measurements of initial velocities at different concentrations of GlcNAc6P), while k_{cat} did not change (see Table 1). However the k_{cat} was reduced to 96 s^{-1} (~66% of the wild-type), while the L and c parameters of the MWC model remained as in the wild-type enzyme (see Table 1). Also the K_i measured (4.3 ± 0.2 μM) for the linear competitive inhibitor (GlcN-ol-6P) in the presence of allosteric activator was similar to the one for the wild-type enzyme (2.43 ± 0.2 μM, Table 1). Therefore, the allosteric properties of the triple mutant used as the starting point for SDL remained as in the wild-type GlcN6P deaminase of *E. coli*.

Kinetics of GlcN6P Deaminase Labeled at Position 164 or 206 with Bimane or Dansyl-amidoethyl Moiety. To obtain a system with cysteine reactivity to the positions 164 or 206, site-directed mutagenesis was carried out from the previously described triple mutants (C118S/C228S/C239S); the mutants obtained, H164C/C118S/C228S/C239S and S206C/C118S/C228S/C239S, were named as 164C-GlcN6P deaminase and 206C-GlcN6P deaminase, respectively. Labeling efficiency of the mutant enzymes with mBBr or dansyl-amidoethyl-MTS was 98% as determined by their reactivity to DTNB (see Materials and Methods). Kinetics of deaminase activity of labeled proteins showed a reduction of velocity of 50%

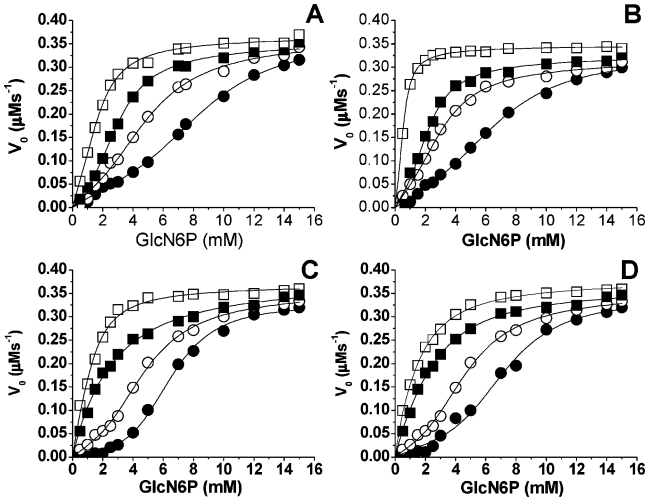

FIGURE 2: Initial velocity curves for the deaminase reaction for 164C-GlcN6P and 206C-GlcN6P deaminases chemically modified with mBBr and dansyl-amidoethyl-MTS at different fixed concentration of the allosteric ligand. Initial velocities were expressed in micromolars of fructose produced per second per mole of hexameric enzyme and were measured at 30 °C in 50 mM Tris-HCl (pH 7.5). (A) Bimane-164C-GlcN6P deaminase; (B) dansyl-amidoethyl-164C-GlcN6P deaminase; (C) bimane-206C-GlcN6P deaminase; and (D) dansyl-amidoethyl-206C-GlcN6P deaminase. The fixed concentrations of the allosteric activator (GlcNAc6P) were 0 (●), 0.01(○), 0.5 (■), and 1mM (□) for all protein preparations. The curves corresponded to the fit of the data to the MWC model (*20*) by nonlinear regression.

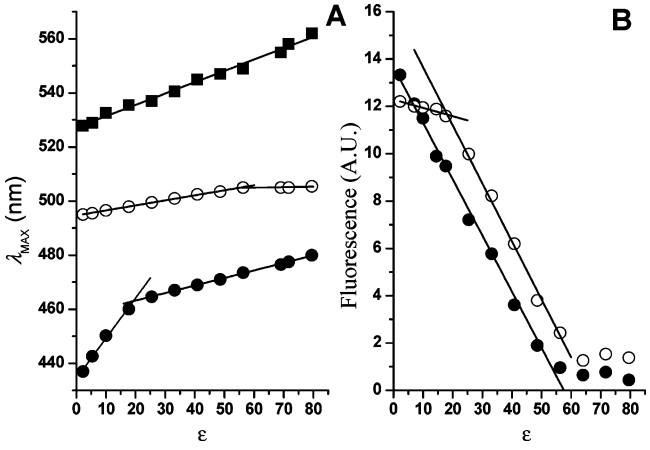

FIGURE 3: Dependence of fluorescence emission spectra of bimane−cysteine and dansyl-amidoethyl−cysteine with the solvent polarity (ϵ) of the medium. The fluorescence spectra were recorded at 30 °C in 50 mM Tris-HCl (pH 7.5) with mixtures of buffer/dioxane to generate the different solvent polarities. (A) Linear correlations on λ_{max} of the fluorescence emission spectra at different dielectric constant values generated by mixtures of buffer/dioxane for bimane−cysteine (●) and for the two maxima of the fluorescence emission spectra (λ_{max1}, ○, and λ_{max2}, ■) of dansyl-amidoethyl−cysteine. (B) Linear correlations for the changes in the intensity of fluorescence emission (in arbitrary units) of dansyl amidoethyl−cysteine at different dielectric values generated by mixtures of buffer/dioxane. Intensity of fluorescence emission for the first maximum (○) and for the second maximum (●).

as compared to wild-type enzyme. Nevertheless, positive homotropic and heterotropic activations were obtained when initial velocities were followed at different GlcNAc6P concentrations (Figure 2). Kinetic data adjusted to the MWC model indicated a *K*-type allosteric activation pattern: $K_{0.5}$ for substrate diminished from ∼5 mM in the absence of allosteric activator to ∼0.5 mM in the presence of allosteric activator (Figure 2 and Table 2), and the k_{cat} of the four mutant enzymes did not change; their values were between 70 and 72 s^{-1}. The *L* parameter varied from 0.7×10^6 to 1.0×10^6; and the *c* parameter ranged from 0.02 to 0.04, which indicated that the equilibrium between T- and R-conformers is remarkably displaced toward the T-conformer in the absence of ligands as in the wild-type enzyme. The K_i measured for the competitive inhibitor GlcN-ol-6P with these enzymes was similar to the value reported (*12*, Table 2). Therefore, GlcN-ol-6P was used as a ligand of the active site to induce conformational changes instead of the substrate (GlcN6P), due to the kinetic and crystallographic evidences that GlcN-ol-6P induce the T to R transition (*13*, *14*).

Fluorescence of Bimane or of Dansyl-amidoethyl Attached to Cysteines Is Dependent on Solvent Polarity. To correlate the changes on the fluorescence emission spectra of the labels at positions 164 or 206 of GlcN6P deaminase with the T to R transition, the solvent polarity dependence of the spectral properties of the mBBr and dansyl-amidoethyl-MTS attached to cysteine were tested prior to the chemical modification the enzyme. The spectroscopic properties of mBBr have been described (*6*, *27*); however, we include the mBBr characterization for comparison purposes. Correlation curves of the change in the maximal emission wavelength (λ_{max}) with the solvent polarity of the medium (Figure 3A) were obtained with mixtures of dioxane ($\epsilon = 2.2$) and water ($\epsilon = 79.5$). Fluorescence emission spectra of bimane−cysteine showed a shift in the λ_{max} from ∼440 to 475 nm (λ_{exc} 381 nm) when solvent polarity was increased (Figure 3A), and two intervals of linear correlations were observed (*6*, *27*); there was no linear correlation with fluorescence intensity (data not

Table 2: Kinetic Parameters of the Mutants of GlcN6P Deaminase of *E. coli*, Labeled with mBBr and Dansyl-amidoethyl-MTS

	k_{cat} (s^{-1})[a]	K_M (mM)[b]	$K_{0.5GlcN6P}$ (mM)[c]	k_{cat}/K_M	L ($\times 10^6$)[d]	c[d]	$K_{i\ GlcN\text{-}ol\text{-}6P}$ (μM)[e]
bimane-164C GlcN6P deaminase	71.6 ± 0.08	0.52 ± 0.014	5.1 ± 0.01	1.30×10^5	1.0 ± 0.05	0.042 ± 0.003	3.6 ± 0.5
dansyl-164C GlcN6P deaminase	70.6 ± 0.1	0.51 ± 0.02	5.2 ± 0.02	1.38×10^5	0.8 ± 0.06	0.020 ± 0.002	4.1 ± 0.6
bimane-206C GlcN6P deaminase	69.5 ± 0.07	0.52 ± 0.018	4.6 ± 0.05	1.33×10^5	0.7 ± 0.03	0.038 ± 0.004	3.5 ± 0.4
dansyl-206C GlcN6P deaminase	70.9 ± 0.11	0.49 ± 0.02	5.1 ± 0.04	1.44×10^5	0.9 ± 0.07	0.033 ± 0.002	3.8 ± 0.6

[a] Data calculated from the fitted MWC model (*20*) by nonlinear regression. [b] Data calculated from the fitted Michaelis−Menten equation in the saturating concentrations of the allosteric activator. [c] Data calculated from the fitted Hill equation in absence of the allosteric activator. [d] Data calculated from the fitted MWC equation in the absence of the allosteric activator. [e] Data calculated from the fitted linear competitive equation in the presence of 2 mM of the activator. All constants and deviations standards were calculated from al least three experiments.

shown). Dansyl-amidoethyl−cysteine showed two maxima in its fluorescence emission spectra: the λ_{max1} which was shifted from ~490 to 505 and the λ_{max2} which was shifted from ~530 to 560 nm when the solvent polarity of the medium was increased (λ_{exc} 341 nm). For the first peak, two intervals of linear correlation of λ_{max} with solvent polarity were observed, while for the second peak (λ_{max2}), one linear correlation was found (Figure 3A). The correlations between solvent polarity and fluorescence intensity showed two linear correlations for the first maximum and one linear correlation for the second maximum (Figure 3B). No further changes in the fluorescence intensity were observed at values higher than ~50 in the dielectric constant of the medium (Figure 3B). It is noteworthy that the ratio of fluorescence intensity between the two peaks observed for dansyl-amidoethyl−cysteine was inverted at values of the dielectric constant lower than 10; the ratio of fluorescence intensity of the first peak with respect to the second peak was >1 at values higher than 10 of the dielectric constant, while at values lower than 10, the ratio was <1. Therefore, both fluorophores seem to be excellent labels to correlate the solvent polarity of the medium with measurable changes in the spectroscopic parameters (*6*, 27). In summary, the observed relationships for linear correlations were, for bimane−cysteine, $\lambda_{max} = 1.63\ (nm/\epsilon)\ D + 434.5$ nm (for ϵ between ~2 and 18), $\lambda_{max} = 0.278\ (nm/\epsilon)\ D + 457.3$ nm (for ϵ between ~18 and 60) and, for dansyl-amidoethyl−cysteine, $\lambda_{max1} = 0.185\ (nm/\epsilon)\ D + 494.2$ nm (for the ϵ between ~2 and 56), $\lambda_{max2} = 0.419\ (nm/\epsilon)\ D + 527$ nm (for the ϵ between ~2 and 80), where D is the dielectric constant.

Changes in Spectra of Fluorescence on Labeled Positions with Bimane Moiety upon Addition of Active Site or Allosteric Ligands at Saturation. The experimental advantage of incorporating fluorophores such as mBBr or dansyl-amidoethyl-MTS is that the wavelength of excitation (381 or 341 nm, respectively) does not interfere with the intrinsic fluorescence of proteins, except for a possible quenching effect of trypthophan on bimane moiety when both residues are less than 10 Å apart from each other (*7*). Nevertheless, position 164 is located at more that 10 Å from the closer trypthophan (residue 224) and is located at 14.7 Å from the NE2 residue of the His143 at the active site and 20.2 Å away from the NH2 residue of the Arg158 from the allosteric site in the closer distance. Also, addition of GlcN-ol-6P (1 mM) or of GlcNAc6P (5 mM) to cysteine−bimane induced no changes in fluorescence emission (data not shown); therefore, fluorescence changes observed during ligand titration must be directly correlated to the changes in the microenvironment of the labeled residues of the protein. Emission spectrum of fluorescence of bimane-164C-GlcN6P deaminase showed a λ_{max} of 475 in the absence of ligands and was shifted to 472 nm after addition of the active site ligand (GlcN-ol-6P) at saturating concentrations, or to 468 nm after addition of the allosteric site ligand (GlcNAc6P) at saturating concentrations (Figure 4A). For the enzyme labeled with bimane at position 206 (bimane-206C-GlcN6P), the λ_{max} shifted from 477 nm (in the absence of ligand) to 474 nm in the presence of GlcN-ol-6P at saturating concentrations or to 472 nm in the presence of GlcNAc6P at saturating concentrations (Figure 4B). Therefore, both positions 164 and 206 sensed a reduction of microenvironment polarity when the R-conformer was induced by either ligand, and according to our

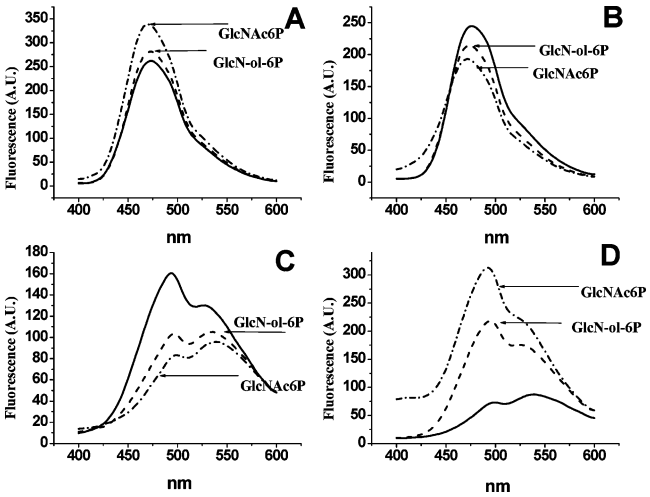

FIGURE 4: Steady state of fluorescence emission spectra of the fluorescent-labeled GlcN6P deaminases with bimane or dansyl-amidoethyl moieties in the presence of the ligands of the active site or the allosteric site at saturation. The fluorescence spectra were recorded at 30 °C, in 50 mM Tris-HCl (pH 7.5). For the four fluorescent-labeled proteins, the saturating concentrations of GlcNAc6P were 2 mM and of GlcN-ol-6P were 0.3 mM. (A) Bimane-164C-GlcN6P deaminase; (B) bimane-206C-GlcN6P deaminase; (C) dansyl-amidoethyl-164C-GlcN6P deaminase; and (D) dansyl-amidoethyl-206C-GlcN6P deaminase.

polarity calibration, the microenvironment polarity changed from ~55 units of the dielectric constant in the absence of ligands to ~48 in the presence of GlcN-ol-6P or ~43 in the presence of GlcNAc6P (Figure 3). Both preparations presented maximal changes in their fluorescence emission spectra after GlcNAc6P addition. Additionally, the change in the λ_{max} in the fluorescence emission produced by the allosteric activator was not further modified when the ligand of the active site was added. On the contrary, the fluorescence spectra produced by the active site ligand GlcN-ol-6P were modified by addition of GlcNAc6P, giving rise spectra similar to the ones obtained with the allosteric ligand alone (Figure 4). The differences in the maximal change in the λ_{max} of fluorescence emission indicate different microenvironments in the labeled positions when the allosteric transition was induced from the active site or from the allosteric site.

Changes in Spectra of Fluorescence on Labeled Positions with Dansyl-amidoethyl Moiety upon Addition of Active Site or Allosteric Ligands at Saturation. Position 206 is 15.3 Å away from the NE2 residue of the His143 of the active site and is 27 Å away from the NH2 residue of Arg158 of the allosteric site in the closer distance. Addition of GlcN-ol-6P (1 mM) or GlcNAc6P (5 mM) did not change the fluorescence emission of the dansyl-amidoethyl−cysteine (data not shown). Therefore, the variations in fluorescence emission spectra were also due to changes in the environment of the labeled positions of the protein. Dansyl-164C-GlcN6P deaminase in the absence of ligands exhibited two maxima in its fluorescence spectra at 493 (λ_{max1}) and 530 (λ_{max2}) nm (λ_{exc} of 341 nm); addition of GlcN-ol-6P at saturating concentrations shifted the two λ_{max} values of the emission spectra to 496 and 536 nm, respectively; addition of GlcNAc6P at saturating concentrations shifted the two λ_{max} values to 498 and 538 nm, respectively (Figure 4C). The shift in the λ_{max} suggested that the dansyl-164C-GlcN6P deaminase sensed an increase in the microenvironment

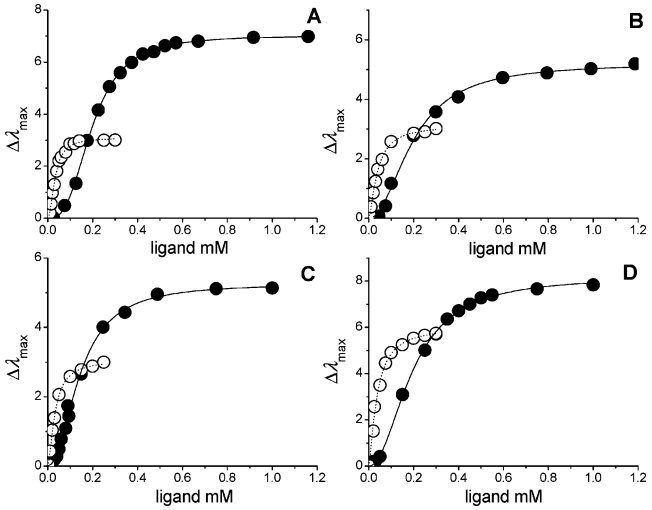

FIGURE 5: Titration of the allosteric site and the active site of the fluorescent-labeled GlcN6P deaminases. Titrations were measured by the changes in the absolute value of the difference of the maxima of the fluorescence emission spectra in the absence of the ligand minus in the presence of the ligand ($\Delta\lambda_{max}$). The titration experiments were made with the ligand of the allosteric site (GlcNAc6P, ●) or the ligand of the active site (GlcN-ol-6P, ○), recorded at 30 °C in 50 mM Tris-HCl (pH 7.5). (A) Changes of $\Delta\lambda_{max}$ for bimane-164C-GlcN6P deaminase; (B) changes of $\Delta\lambda_{max}$ for dansyl-amidoethyl-164C-GlcN6P deaminase; (C) changes of $\Delta\lambda_{max}$ for bimane-206C-GlcN6P deaminase; and (D) changes of $\Delta\lambda_{max}$ for dansyl-amidoethyl-206C-GlcN6P deaminase. The curves corresponded to the fit of the data to the Hill equation by nonlinear regression.

polarity in the presence of the ligands (conformer R). This contrasted strongly with the behavior observed for the bimane-164C-GlcN6P deaminase. This discrepancy in the solvent polarity reported by each fluorophore is analyzed in terms of the crystallographic structure (see Discussion). For dansyl-206C-GlcN6P deaminase in the absence of ligands, the two λ_{max} values were 500 and 538 nm, and after addition of GlcN-ol-6P at saturating concentrations, the λ_{max} values were shifted to 494 and 529 nm, respectively. In the presence of GlcNAc6P at saturating concentrations, the two λ_{max} values were shifted to 492 and 528 nm, respectively (Figure 4D). The estimated value of relative polarity from our correlation was close to 10 in the dielectric constant of the microenvironment of the labels (in absence of ligands) but decreased to 5 and 3 in the presence GlcN-ol-6P and GlcNAc6P, respectively (Figure 3A). These data indicated a reduction in the microenvironment polarity at position 206 when the R-conformer was induced. Higher changes in the fluorescence spectra were observed in the presence of the allosteric ligand than with the ligand of the active site. Also, addition of the allosteric ligand to the enzyme saturated with the active site ligand always generated a change in the fluorescence spectra (increasing the values obtained by the allosteric ligand alone). These results were consistent with those obtained with the bimane-206C-GlcN6P enzyme and suggest differences in the microenvironment polarity detected by the fluorescent labels when the T to R transition was induced by either ligand.

Titration of the Active Site or Allosteric Ligands Measured by the Changes in λ_{max} of Fluorescent-Labeled Mutants. Figure 5 and Table 3 show the changes in the fluorescence spectra of labeled enzymes titrated with the ligands of the active site or the allosteric site. The changes in the absolute value of λ_{max} of fluorescence emission were used as the correlation parameters for the titration with ligands with the labeled enzymes to avoid negative values (the shifts in the λ_{max} were to lower wavelengths when the relative polarity diminishes). For dansyl-164C-GlcN6P deaminase and dansyl-206C-GlcN6P deaminase, both $\Delta\lambda_{max1}$ (first peak) and the changes in fluorescence intensity gave the same correlation parameters for the titration with the active or the allosteric site ligands. In general, the $K_{0.5}$ for GlcNAc6P ranged from ~194 μM (for both labeled proteins of 164C-GlcN6P deaminase and dansyl-206C-GlcN6P deaminase) to 143 μM for bimane-206C-GlcN6P deaminase (see Figure 5 and Table 3). These values are 4−5 times higher than the K_d reported for GlcNAc6P from direct binding to the wild-type enzyme (*12*, *28*). Therefore, steric effects produced by incorporation of fluorescent labels at the protein interface may disturb propagated critical contacts that originate the reduction in the affinity for the allosteric site. $K_{0.5}$ for GlcN-ol-6P for all labeled mutants was ~30 μM (Table 3), which is in agreement with the K_d obtained by direct binding in the absence of allosteric ligand (*28*). The Hill parameters were higher for allosteric site ligand ranging from 3 for 164-GlcN6P deaminase to 2 for the other three enzyme preparations, while Hill values for GlcN-ol-6P were notably less cooperative, ranging between 1.84 (for bimane-164-GlcN6P deaminase) to ~1.4 in the other three fluorescent-labeled preparations. The perturbation created by the introduction of labels maintains an allosteric activation of *K*-type as in

Table 3: Titration by the Active or the Allosteric Site Ligands to the Mutants of GlcN6P Deaminase Labeled with Fluorophores and Measured by Changes in the Absolute Value of the Difference of the λ_{max} of Fluorescence Emission Spectra in the Absence of Ligand Minus in the Presence of Ligand ($\Delta\lambda_{max}$)

		allosteric site ligand, GlcNAc6P			active site ligand, GlcN-ol-6P	
	$\Delta\lambda_{max}$ (nm)[a,b]	$K_{0.5GlcNAc6P}$ (mM)[c]	Hill number[c]	$\Delta\lambda_{max}$ (nm)[a,b]	$K_{0.5GlNol6P}$ (mM)[c]	Hill number[c]
bimane-164C GlcN6P deaminase	7.1	0.194 ± 0.005	2.90 ± 0.08	3.08	0.032 ± 0.009	1.84 ± 0.09
dansyl-164C GlcN6P deaminase	5.03	0.198 ± 0.009	2.15 ± 0.12	3.01	0.038 ± 0.004	1.36 ± 0.07
bimane-206C GlcN6P deaminase	5.05	0.143 ± 0.004	2.06 ± 0.01	3.0	0.032 ± 0.003	1.42 ± 0.012
dansyl-206C GlcN6P deaminase	8.3	0.192 ± 0.015	2.09 ± 0.016	6.0	0.035 ± 0.004	1.39 ± 0.014

[a] Data were calculated from a Hill equation in which $(\lambda_{max}x^n)/(K_d + x^n)$; x is the wavelength in nanometers. [b] Absolute value of the difference of λ_{max} of the fluorescence emission spectra in the absence of ligand minus λ_{max} of the fluorescence emission spectra in the presence of ligand. All constants and deviations standards were calculated from al least three experiments. [c] Data were calculated from the titration curves adjusted to the Hill equation by nonlinear regression.

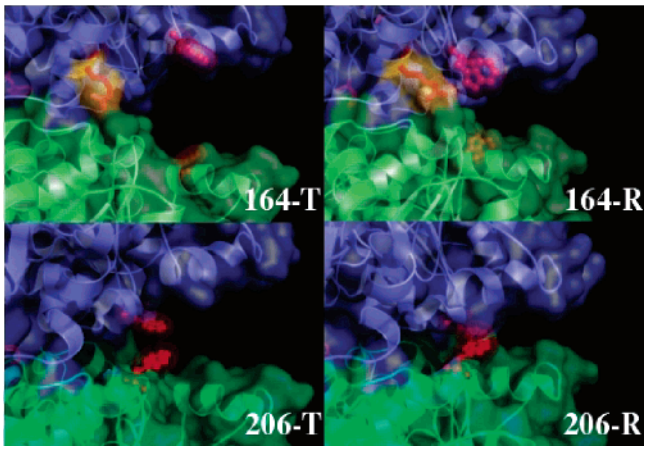

FIGURE 6: Model of the three-dimensional structure of GlcN6P deaminase to indicate the differential interaction of the residues at the interface of two trimers among the T to R transition. The residues 164 and 206 were in red in the T (left) state and R (right) state, respectively; the Arg253 in orange (see Discussion) residues were indicated; also, the solvent-accessible surface is indicated to appreciate the closure process from T to R states. Residues His164 or Ser206 were mutated "in silico" for trypthophan residue as described in Materials and Methods. Molecular graphic representations were made with PyMOL program (*23*).

the wild-type enzyme, and the binding constants obtained by changes in fluorescence spectra correlated with the kinetic constants measured in this work and previous studies (*11*, *12*). Therefore, the process studied here throughout spectral changes (λ_{max}) of the fluorescent labels when the R-conformer was induced from the active or from the allosteric site indicated structural differences in the rearrangements at the interface of the two trimers that form the enzyme.

DISCUSSION

Glucosamine 6-phosphate deaminase of *E. coli* has two described conformers by the crystallographic studies that apparently correlate with the kinetic activation described for its ligands: a T-conformer in the absence of ligands and an R-conformer in the presence either allosteric ligand (GlcNAc6P) or the active site ligand (GlcN-ol-6P, in the presence of inorganic phosphate *13*, *14*). The homotropic activation of the substrate with a distinctive sigmoidal shape of initial velocity of GlcN6P deaminase is explained by a change in affinity to the substrate when the equilibrium is shifted toward the R-conformer (Figure 2). Also, heterotropic activation by the allosteric ligand (Figure 2) produces a conformational change in the enzyme toward its R-conformer (Figure 6). Kinetics of this enzyme has been satisfactorily described by the MWC equation (*20*); however, the renewed interest to correlate the relations between the structure and function of the allosteric proteins have shown that neither the simple two-state model nor the sequential model described the network of allosteric communications of the phosphofructokinase of *E. coli* (*14*) and *Bacillus stearothermophilus* (*15*), systems that have been previously described by the two-state allosteric model. Also, recent kinetic studies of encapsulated hemoglobin in silica gels were explained by an extension of the two-state model, in which a preequilibrium between two functionally different tertiary states, rather than quaternary conformations, plays the central role in the allosteric regulation of the hemoglobin (*29*). Therefore, it is fundamental to develop methods that allow quantitative determinations of the dynamics of the allosteric systems in solution. Here, fluorescent labeling of GlcN6P deaminase at the residues of the interface between two trimers was performed, to monitor quaternary structure modifications in solution without interfering with important residues at the active or the allosteric sites that may perturb the equilibrium between the T to R transition and test if the conformation of the R′-state induced from the active site indicates structural differences to the R-conformer induced from the allosteric site.

Quaternary Changes of the Structure of GlcN6P Deaminase upon Binding of Ligands at Positions 164 and 206. Histidine 164 is located in the base of the region denominated the lid of the active site (residues 154−184) at the α-helix 7 (Figure 6), facing the interface between trimers. At the T-conformer, position 164 has only intramonomeric contacts, but in the R-conformer, it establishes a van der Waals contact with Arg253 and Glu257 of the contiguous subunit (across a symmetry axis of order two). Arg253 also establishes different contacts: when the enzyme is in the T-conformer, it has a contact with the Glu241, but in the R-conformer, the guanidine moiety is rotated to create a new van der Waals contact with Glu257 and His164. Also, the distance from the NE residue of Arg253 to the NE2 residue of His164 is reduced from 12.5 to 4.8 Å when the T-state is shifted to the R-state.

Ser206 is located in helix 9 that belongs to the external module of the α/*β* structure described in ref *14*. This residue is also facing the interface of two trimers of the hexameric structure. Ser206 in the T-conformer has only intrasubunit interactions, but in the R-conformer, it establishes a closer van der Waals contact with Asp165 of the contiguous subunit (across a symmetry axis of order three). Asp165 also establishes an ionic contact with Lys250 in the R-conformer, which may stabilize this interaction.

Since residues 164 and 206 create new contacts with contiguous subunits upon the T to R shift, the microenvironment of the fluorescent labels introduced at these positions must change accordingly (Figure 6). To gain more insights on the microenvironment changes around residues 164 and 206, surface solvent accessibility was estimated by the program NACCESS (*25*) based on the crystallographic structures of the T- and R-conformers. Because the size of a bimane attached to the protein is about the size of the trypthophan (*6*), residues 164 and 206 were modeled as energy-minimized trypthophans (see Materials and Methods). Solvent accessibility calculations for residue 164 indicated a reduction of 36.6 Å^2 from T-conformer (153.3 Å^2) to R-conformer (116.7 Å^2), and for residue 206, a reduction of 56.7 Å^2 from T-state (152.1 Å^2) to R-conformer (96.2 Å^2). A similar reduction was determined for the original residues His164 and Ser206. The reduction of microenvironment polarity at positions 164 and 206 measured by fluorescent labels correlated with a reduction in solvent accessibility calculated from crystallographic structures (Figure 6), except for the dansyl-164C-GlcN6P deaminase, in which the microenvironment polarity increased after ligand addition. Emission spectra of fluorophore labels attached to proteins are subject to perturbations of the fluorescence signal such as the effect of hydrogen bonds or electrostatic interactions (*6*, *7*). Also, the chemical nature of the label may influence the interval of microenvironment polarity detected; for the

bimane-labeled proteins, the value of the microenvironment polarity detected was ~50 in the dielectric constant of the environment, while for dansyl-amidoethylated protein, it was ~10. A possible explanation of the anomalous change for solvent polarity detected by the dansyl-164C-GlcN6P deaminase is that position 164 of the R-conformer may establish a polar contact with Arg253. This interaction was not modified even by the trypthophan substitution made "in silico" (Figure 6). The dansyl-amidoethyl moiety may be more sensitive to detect the polar contacts than bimane. Also, the effect of burying position 164 in the R-conformer could contribute to the lack of detection of this polar contact with bimane but not with dansyl-amidoethyl label. Further studies are required to understand the fluorescence-induced differential effect.

The changes in the fluorescence spectra reflect rearrangements of the enzyme during T to R transition. In fact, the kinetic constants obtained for the labeled proteins (Tables 2 and 3) correlate with the previous kinetic studies (*10*−*12*). The only appreciable effect on the kinetic parameters was a reduction of k_{cat} of the labeled proteins (approximately 50% of wild-type activity). This may be due to a steric perturbation of the interface contacts during the allosteric transition. Also, it is important to note that the main decrease in enzyme activity was attributed to the replacement of serines by cysteines (33% of the original activity) and, to a minor extent, to the chemical modification (Tables 1 and 2). Although SDL does not perturb the secondary structure of proteins (*6*−*9*), the introduction of new residues, combined with the chemical moieties, disrupts the precise three-dimensional contacts required for maximal velocity. The energy perturbation generated by introduction of chemical groups such as a bimane moiety was minimized at position 164 or 206, because both residues were exposed ≥40 Å^2 in both conformers. The energy destabilization is less than 1.5 kcal for residues labeled with mBBr if the solvent accessible area is ≥40 Å^2, as observed on lysozyme T4 (*7*). This is an important requisite that should be taken in consideration in SDL studies. For GlcN6P deaminase, chemical modifications of residues with less that 50 Å^2 of exposed solvent surface in any of the two enzyme conformers produced loss of activity or reduction in the yield of protein production (data not shown).

The Differences in the Microenvironment Detected by the Fluorescent Labels Indicated Structural Differences in the Conformation of the R-State When Is Induced from the Active Site or from the Allosteric Site. A similar behavior of the changes of the fluorescence spectra was observed when GlcN-ol-6P or GlcNAc6P was added. In all cases, the microenvironment polarity was reduced with both ligands (λ_{max} was shifted to lower wavelengths), except for dansyl-164C-GlcN6P deaminase, in which an increase in the microenvironment polarity was obtained with any ligand. Altogether, the data are in agreement with the induction of T to R transition upon interaction with either ligand. Nonetheless, the changes in the fluorescence spectra obtained with the active site ligand was always modified by the allosteric ligand (to the level of the GlcNAc6P alone), but not vice versa. The spectra of fluorescent labels introduced at GlcN6P deaminase were very sensitive to the changes in local polarity due to the high quantum efficiency (0.145 for bimanated proteins and 0.09 for dansyl-amidoethylated proteins, as compared with 0.007 for the two trypthophans in the wild-type enzyme). For example, note that the small changes in λ_{max} were detected during the ligand titration, despite the wider slit for the emission channel of the spectrofluorometer. Therefore, the microenvironment generated at the R′-conformer from the active site ligand is different to the one generated from the allosteric ligand. Comparison of the crystallographic structures between the two conformers indicated that the upper and lower trimers of the hexameric structure rotate 13.1° around a three-fold axis of symmetry; accordingly, it is likely that the conformational changes associated with GlcN-ol-6P are not as pronounced as the conformational changes (or rotation between the two trimers) associated with GlcNAc6P. Also, crystals of GlcN6P deaminase on the T-conformation are easily disintegrated by the addition of the allosteric ligand. In contrast, addition of GlcN-ol-6P did not modify the crystals of the T-enzyme; this was attributed to the fact that crystalline contacts could have hindered the T to R transition (*13*, *14*). Here, we take this structural information as another evidence of the different role for the ligands to stabilize the R-conformer. In addition, Arg158 and Lys160 of one monomer, together with the terminal amino group of the neighboring subunit, bind the phosphate moiety of the allosteric activator at the R-state (*13*, *14*). Therefore, the R-conformer induced by the active site ligand may not stabilize the positive charges of the allosteric site unless phosphate is added. This idea correlates with the data obtained in the present work: bigger changes and cooperative effects were observed in the fluorescence spectra in the presence of the allosteric ligand as compared with smaller and noncooperative effects observed in the presence of the active site ligand (Figure 5 and Table 3).

Concluding Remarks. The data presented here indicate that the R-conformer induced from the active site is different from the one induced from the allosteric site for the GlcN6P deaminase, as suggested by the differences at the microenvironment of the interface of two trimers of the hexameric enzyme studied by SDL. This information contrast with the two-state model proposed from the crystallographic structures of the R-conformer in the presence of either ligand. Nonetheless, it was not surprising to have a different contribution of either ligand to the conformation of the R-state when fluorescent techniques were applied, due to the inability of crystallographic techniques to reveal or stabilize the diversity of the conformers in solution. These data are in agreement with recent works that show the complexity of the allosteric enzymes regulation (*5*, *29*), in which new intermediates of the crystallographic structures between the T- and R-states were reported, from a single mutant that destabilizes the native R-state of the aspartate transcarbamylase (*30*). Fluorescence studies of fructuose-1,6-biphosphatase indicated that the R-state is part of a conformational family of the T-state (*4*). Also, a recent study that combines kinetics and trypthophan fluorescence techniques for the GlcN6P deaminase of *E. coli* indicated that the pathway of quaternary changes propagation from the active site is different of the pathway propagation from the allosteric site (*28*). Ligand-induced quaternary structural rearrangements of allosteric enzymes are an important task that should be undertaken with a combination of techniques in solution, to refine and complement the information obtained from crystallographic

approaches for the advance in the dynamics of the allosteric proteins.

ACKNOWLEDGMENT

The authors thank Dr. Mario L. Calcagno for introducing to us the GlcN6P deaminase and for helpful discussion, Dr. Jacqueline A. Plumbridge for the *E. coli* strain (IBPC590), Dr. Diego Gonzalez-Halphen for critical reading of the manuscript, and Veronica Cortés-Avilés for technical assistance.

REFERENCES

1. Hammes, G. G. (2002) Multiple conformational changes in enzyme catalysis, *Biochemistry 41*, 8221−8228.
2. Luque, I., Leavitt, S. A., and Freire, E. (2002) The linkage between protein folding and functional cooperativity: two sides of the same coin? *Annu. Rev. Biophys. Biomol. Struct. 31*, 235−256.
3. Volkman, B. F., Lipson, D., Wemmer, D. E., and Kern, D. (2001) Two state allosteric behavior in single domain signaling protein, *Science 291*, 2449−2433.
4. Nelson, S. W., Iancu, C. V., Choe, J. Y., Honzatko, R. B., and Fromm, H. J. (2000) Tryptophan fluorescence reveals the conformational state of a dynamic loop in recombinant porcine fructose-1,6-bisphosphatase, *Biochemistry 39*, 11100−11106.
5. Kern, D., and Zuiderberg, E. R. P. (2003) The role of dynamics in allosteric regulation, *Curr. Opin. Struct. Biol. 13*, 748−757.
6. Mansoor, S. E., McHaourab, H. S., and Farrens, D. L. (1999) Determination of protein secondary structure and solvent accessibility using site-directed fluorescence labeling. Studies of T4 lysozyme using the fluorescent probe monobromobimane, *Biochemistry 38*, 16383−16393.
7. Mansoor, S. E., McHaourab, H. S., and Farrens, D. L. (2002) Mapping proximity within proteins using fluorescence spectroscopy. A study of T4 lysozyme showing that tryptophan residues quench bimane fluorescence, *Biochemistry 41*, 2475−2484.
8. Hubbell, W. L., Gross, A., Langen, R., and Lietzow, M. A. (1998) Recent advances in site-directed spin labeling of proteins, *Curr. Opin. Struct. Biol. 8*, 649−656.
9. Perozo, E., Cortes, D. M., and Cuello, L. G. (1998) Three-dimensional architecture and gating mechanism of a K^+ channel studied by EPR spectroscopy, *Nat. Struct. Biol. 5*, 459−469.
10. Calcagno, M. L., Campos, P. J., Mulliert, G., and Suástegui, J. (1984) Purification, molecular and kinetic properties of glucosamine 6-phosphate isomerase (deaminase) from *Escherichia coli*, *Biochim. Biophys. Acta 787*, 165−173.
11. Altamirano, M. M., Plumbridge, J. A., Horjales, E., and Calcagno, M. L. (1995) Asymmetric allosteric activation of *Escherichia coli* glucosamine-6-phosphate deaminase produced by replacements of Tyr 121, *Biochemistry 34*, 6074−6082.
12. Montero-Morán, G. M., Horjales, E., Calcagno, M. L., and Altamirano, M. M. (1998) Tyr254 hydroxyl group acts as a two-way switch mechanism in the coupling of heterotropic homotropic effects in *Escherichia coli* glucosamine-6-phosphate deaminase, *Biochemistry 37*, 7844−7849.
13. Oliva, G., Fontes, M. R. M., Garrat, R. C., Altamirano, M. M., Calcagno, M. L., and Horjales, E. (1995) Structure and catalytic mechanism of glucosamine 6-phosphate deaminase of *Escherichia coli* at 2.1 Å resolution, *Structure 3*, 1323−1332.
14. Horjales, E., Altamirano, M. M., Calcagno, M. L., Garrat, R. C., and Oliva, G. (1999) The allosteric transition of glucosamine 6-phosphate deaminase: the structure of T-state at 2.3 Å resolution, *Structure 7*, 527−537.
15. Fenton, A. W., and Reinhart, G. D. (2002) Isolation of a single activating allosteric interaction in phosphofructokinase from *Escherichia coli*, *Biochemistry 41*, 13410−13416.
16. Ortigosa, A. D., Kimmel, J. L., and Reinhart, G. D. (2004) Disentangling the web of allosteric communication in a homotetramer: heterotropic inhibition of phosphofructokinase from *Bacillus stearothermophilus*, *Biochemistry 43*, 577−586.
17. Altamirano, M. M., Plumbridge, J. A., Hernandez-Arana, A., and Calcagno, M. (1991) Secondary structure of *Escherichia coli* glucosamine-6-phosphate deaminase from an amino acid sequence and circular dichroism spectroscopy, *Biochim. Biophys. Acta 1076*, 266−277.
18. Smith, P. K., Krohn, R. I., Hermanson, G. T., Mallia, A. K., Gartner, F. H., Provenzano, M. D., Fujimoto, E. K., Goeke, N. M., Olson, B. J., and Klenk, D. C. **(**1985) Measurement of protein using bicinchoninic acid, *Anal. Biochem. 150*, 76−85.
19. Kosower, N. S., and Kosower, E. M. (1987) Thiol labeling with bromobimanes, in *Methods in Enzymology* (William, B. J., Owen, W. G., Ed.) pp 76−84, Academic Press, New York.
20. Monod, J., Wyman, J., and Changeux, J. P. (1965) On the nature of allosteric transitions: a plausible model, *J. Mol. Biol. 12*, 88−118.
21. Ellman, G. L. (1958) A colorimetric method for determining low concentrations of mercaptans, *Arch. Biochem. Biophys. 74*, 443−450.
22. Chen, R. (1965) Fluorescence quantum yield measurements: vitamin B6 compounds, *Science 150*, 1593−1595.
23. DeLano, W. L. (2002) The PyMOL molecular graphics system on world wide web, http://www.pymol.org.
24. Brooks, B. R., Bruccoleri, R. E., Olafson, B. D., States, D. J., Swaminathan, S., and Karplus, M. (1983) CHARMM: a program for macromolecular energy, minimization, and dynamics calculations, *J. Comput. Chem. 4*, 187−217.
25. Hubbard, S. J., and Thornton, J. M. (1993) 'NACCESS', computer program, Department of Biochemistry and Molecular Biology, University College London, London, U.K.
26. Altamirano, M. M., Plumbridge, J. A., and Calcagno, M. L. (1992) Identification of two cysteine residues forming a pair of vicinal thiols in glucosamine-6-phosphate deaminase from *Escherichia coli* and a study of their functional role by site-directed mutagenesis, *Biochemistry 31*, 1153−1158.
27. Kosower, E. M., Giniger, R., Radkowsky, A., Hebel, D., and Shusterman, A. (1986) Bimanes 22. Flexible fluorescent molecules. Solvent effects on the photophysical properties of *syn*-bimanes (1,5-diazabicyclo[3.3.0]octa-3,6-diene-2,8-diones), *J. Phys. Chem. 90*, 5552−5557.
28. Bustos-Jaimes, I., Ramírez-Costa, M., De-Anda-Aguilar, L., Hinojosa-Ocaña, P., and Calcagno, M. L. (2005) Evidence for two different mechanisms triggering the change in quaternary structure of the allosteric enzyme, glucosamine-6-phosphate deaminase, *Biochemistry 44*, 1127−1135.
29. Viappiani, C., Bettati, S., Bruno, S., Ronda, L., Abruzzetti, S., Mozzarelli, A., and Eaton, W. A. (2004) New insights into allosteric mechanisms from trapping unstable protein conformations in silica gels, *Proc. Natl. Acad. Sci. U.S.A. 101*, 14414−14419.
30. Stieglitz, K., Stec, B., Baker, D. P., and Kantrowitz, E. R. (2004) Monitoring the transition from the T to the R state in *E. coli* aspartate transcarbamylase by X-ray crystallography: crystal structures of the E50A mutant enzyme in four distinct allosteric states, *J. Mol. Biol. 341*, 853−868.

BI050306O